# Hydrocarbon measurements in the spring arctic troposphere during the ARCTOC 95 campaign

By BJØRN RAMACHER*, JOCHEN RUDOLPH# and RALF KOPPMANN, *Institut für Atmosphärische Chemie, Forschungszentrum Jülich GmbH, 52425 Jülich, Germany*

ABSTRACT

The hydrocarbon measurements made during the ARCTOC 95 field campaign (16 April–10 June 1995) at Ny Ålesund, Spitsbergen (78°55'N, 11°56'E) allow the estimation of Cl and Br atom concentrations during periods of low ozone concentrations in the lower troposphere. In-situ analyses for nonmethane hydrocarbons and selected halocarbons were carried out with two GC-FID/ECD systems allowing a time resolution of about 2 hours and detection limits in the lower ppt range. A third GC was used to monitor the CO mixing ratio with a 5 min time resolution. Additionally, about 70 whole air samples were collected in stainless steel canisters and analysed for hydrocarbons ($C_2$–$C_8$), some halocarbons, methane, CO, and $CO_2$ at the laboratory in Jülich. 15 of those samples were taken at the measurement site, the others were collected on top of Zeppelin Mountain (474 m a.s.l., distance from measurement site 1000 m). In-situ measurements as well as canister samples showed that all nonmethane hydrocarbons were present at low mixing ratios. CO levels were found to be between 100 and 140 ppb showing a nearly constant decrease from April to June. During an ozone depletion event (18–24 April) the hydrocarbon pattern changed drastically. The mixing ratios of alkanes and ethyne decreased together with ozone, whereas benzene, chloromethane, and CO mixing ratios remained nearly constant. From the ratio of NMHC background mixing ratios and those during low ozone periods the time integrated Cl and Br atom concentrations were calculated to some $10^{10}$ molecules·s·cm$^{-3}$ and $5 \cdot 10^{12}$ molecules·s·cm$^{-3}$, respectively.

## 1. Introduction

Since 1985, the phenomenon of tropospheric ozone depletion in the arctic during spring has been observed (Anlauf et al., 1994, Bottenheim et al., 1986, 1990; Oltmans 1989). On time scales varying between hours and days the ozone mixing ratio drops rapidly from normal levels (30–40 ppb) to levels below the detection limit (1 ppb). Because of an anticorrelation of filterable bromine and ozone an ozone destruction mechanism via bromine atoms forming bromine oxide was suggested (Barrie et al., 1988; Finnlayson-Pitts et al., 1990; Fan et al., 1992; Curry et al., 1993; McConnell et al., 1992). This cycle is closed when two bromine oxide radicals react to yield an oxygen molecule and a bromine molecule, which is photolysed subsequently. Later observations showed that some hydrocarbons are depleted in correlation with ozone, too (Kieser et al., 1993; Bottenheim et al., 1990; Jobson et al., 1994; Yokouchi et al., 1994; Solberg et al., 1996). This supported the idea of halogen atoms influencing the tropospheric chemistry during ozone depletion events. Although several field experiments have been launched in the past, details of the reaction pathways are still unsolved. The source and precursors of the halogen atoms are still not identified.

* Corresponding author.

# Present affiliation: York University, North York, Ontario, Canada.

The possibility of photolysis of halogenated organic trace gases has been studied but none of the compounds examined yielded enough halogen radicals to account for the rapid ozone depletions. The purpose of this study was to improve the database of NMHC mixing ratios in order to provide more quantitative information for the suggested radical mechanism.

## 2. Methods

The ARCTOC 95 campaign was conducted at Ny Ålesund, Svalbard (78°55'N, 11°56'E) in Spring 95 (16.4.-10.6.95). Fig. 1 shows a map of the vicinity of Ny Ålesund as well as its location in the arctic. During the ARCTOC 95 campaign a variety of organic trace gases was measured. Table 1 summarizes the measured substances and the analytical techniques used as well as the time of operation.

Nonmethane hydrocarbons (NMHC) as well as carbon monoxide (CO) were measured by in-situ gas chromatography at a hut called "Gruvebadet". Its location is marked in the map (Fig. 1) and was at about 1 km distance from the village of Ny Ålesund. The road to Zeppelin Mountain was close by the hut but not used frequently

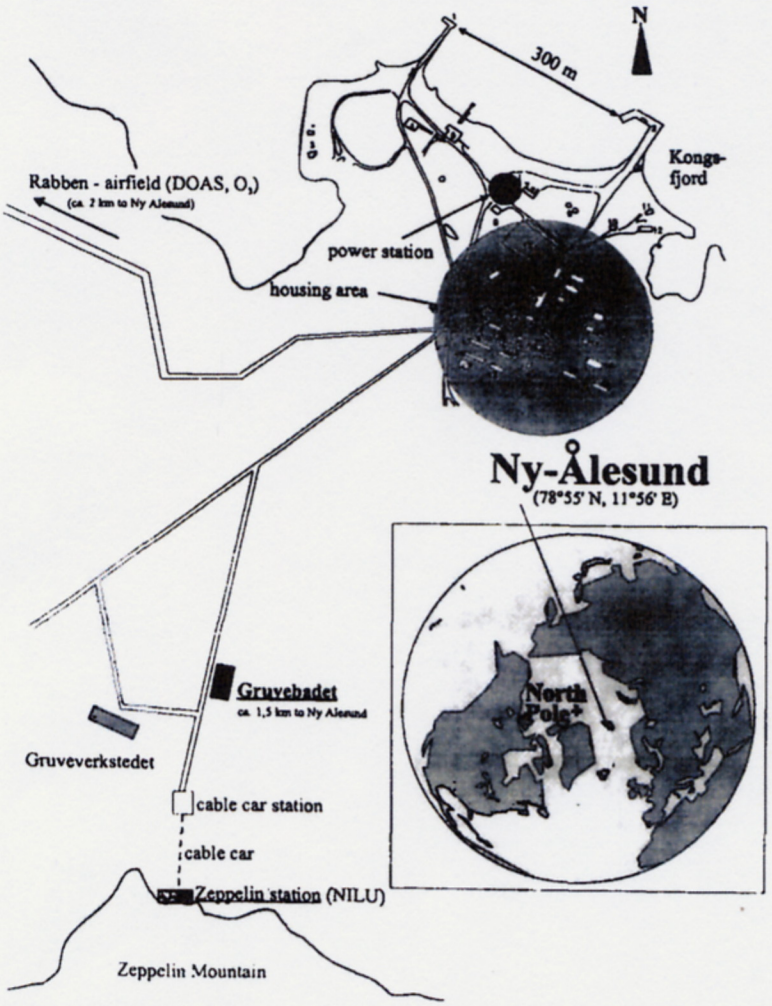


*Fig. 1.* Location of the measurement site.

Table 1. *Measurements performed during ARCTOC 95*

| Method | Sampling location | Time of operation | Sampling frequency |
|---|---|---|---|
| in-situ CO | Gruvebadet | 16.4.95–10.6.95 | 5 min |
| in-situ HC (C2-C7) | Gruvebadet | 19.4.95–31.5.95 | 2 h 40 min |
| in-situ HC/halogenated HC | Gruvebadet | 24.4.95–10.6.95 | 2 h |
| canister HC, halogenated HC, CO, $CO_2$, $CH_4$ | Zeppelin Mountain, Gruvebadet | 19.4.95–10.6.95 | daily (about 70 samples) |

(< 1 vehicle/h). The sample inlet was about 4 m above the roof of the building, which correponds to 8 m above ground level. The intake line (stainless steel tube, 10 mm ID, 7 m length) was continuously flushed with ambient air at a flow of 34 l/min in order to reduce wall losses and contaminations. A fraction of that flow was split off at a virtual impactor by a metal bellows pump. The air samples for NMHC measurements were split off from the low pressure side of that pump, whereas the pressurized air was used for CO analysis.

NMHC (C2-C7 alkanes, alkenes, ethyne and aromatics) were measured by two in-situ gas chromatographs (Siemens Sichromat II) with FID/ECD detection. The instruments are similar to a system described in detail by Rudolph et al. (1986). Schematic drawings of these systems are shown in Fig. 2a–b. The preconcentration system used for both GCs was similar. It consisted of a sample loop (length 20 cm, $d_i = 2$ mm) packed with glass beads (60–80 mesh) immersed into liquid nitrogen. The samples were preconcentrated from 500–4500 mL (STP) of air. After desorption at 120°C the samples were injected onto the GC with the carrier gas (hydrogen 99.999%).

The first system (Fig. 2a), referred to as GC 1, used a Gas Pro GSC PLOT-column (Astec, 0.32 mm ID) for separation. The separation was temperature programmed from 5°C to 250°C at a rate of 5°C/min; carrier gas flow rate was 4 ml/min. The time for one complete analysis was about 2h. This system allowed the analysis of $C_2$–$C_8$ hydrocarbons except ethene, which coelutes with $CO_2$ under the conditions chosen.

In the second system (GC 2, Fig. 2b), the sample was injected onto a 7 m Rtx-1 capillary column (Restek, 0.53 mm ID), which was used to separate the sample into a light ($C_2$–$C_5$) and heavy (> $C_6$) fraction. The light fraction was transferred to a 10 m CW20-m column (Quadrex, 0.53 mm ID) to retain the water, which was vented before elution by switching valve 10. Separation of the light fraction took place on a 50 m aluminium oxide/KCl PLOT-column (J&W, 0.53 mm ID). The heavy fraction was backflushed from the first column during analysis of the light fraction and transferred to a 105 m Rtx-1 column (Restek, 0.53 mm ID) after focusing in a trap cooled to liquid nitrogen temperature. A complete analysis was carried out in 2h 40 min. This system was intended to analyse $C_2$–$C_{10}$ hydrocarbons with optimum resolution in the $C_4$–$C_5$ range. Unfortunately, it was damaged severely during transportation, which allowed measurements only up to $C_5$ hydrocarbons and caused a number of technical problems during the beginning of the campaign leading to gaps in the data set.

The NMHC mixing ratios in the air samples were calculated by comparison with a reference air of known composition. Its mixing ratios were in the order of several ppt to a few ppb and thus comparable to those found at the site. Detection limits range from 2 ppt to 60 ppt depending on the substance, the method, and the size of preconcentrated air sample. Reproducibilities range from 2–38% depending on the compound, but were found to be lower than 10% for most compounds (Table 2).

A commercially available reduction gas analyser (RGA3, Trace Analytical Inc.) was used for CO measurements. The time for one measurement was about 2.5 min. A reference air and the sample were measured alternately to eliminate possible drifts in the detector response. The detection limit and the reproducibility were calculated to 2 ppb and 1.2%, respectively. The linearity of the CO in-situ instrument was checked before the field experiment. The response was found to be linear for CO mixing ratios up to ca. 560 ppb (Ramacher 1997).

Additionally, whole air samples were taken both

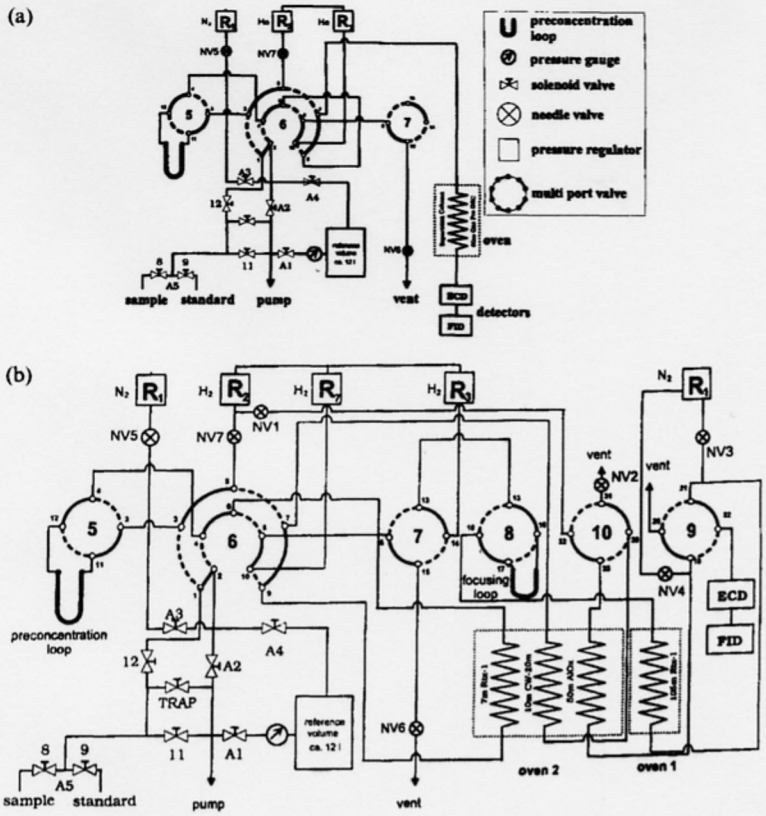


*Fig. 2.* (a,b) Schematic drawings of the gas chromatographic set-ups used in this study, symbols used consistently for both figures.

Table 2. *Detection limits (3σ) and reproducibilities for NMHC measurements during ARCTOC 95 (the relatively poor performance for i-butane and i-pentane in canisters result from incomplete separations)*

| | GC 1 | | GC2 | | Canister | |
|---|---|---|---|---|---|---|
| Compound | Detection limit/ppt | Reproducibility (%) | Detection limit/ppt | Reproducibility (%) | Detection limit/ppt | Reproducibility (%) |
| ethane | 20 | 5 | 9 | 3 | 60 | 7 |
| ethene | 30 | 4 | 11 | 5 | 20 | 4 |
| ethyne | 25 | 7 | 30 | 7 | 15 | 7 |
| propane | 5 | 4 | 10 | 8 | 20 | 2 |
| propene | 4 | 8 | 8 | 8 | 20 | 6 |
| i-butane | 2 | 3 | 6 | 5 | 30 | 15 |
| n-butane | 4 | 4 | 6 | 5 | 15 | 2 |
| i-pentane | 2 | 6 | 5 | 7 | 40 | 38 |
| n-pentane | 2 | 4 | 5 | 8 | 7 | 3 |
| n-hexane | 2 | 16 | | | 6 | 10 |
| benzene | 3 | 4 | | | 10 | 3 |
| toluene | 3 | 11 | | | 8 | 14 |
| $CH_3Cl$ | 20 | 10 | | | 20 | 4 |

on Zeppelin Mountain (474 m a.s.l.) and at the "Gruvebadet" using evacuated 2 l stainless steel canisters. The inlet was 2 m above the roof of the NILU laboratory on Zeppelin Mountain (Braathen et al., 1990) and continuously flushed with a membrane pump. The samples were split off from the low pressure site of that flow and pressurised to 250 kPa by a metal bellows pump. About 55 canisters were filled during the campaign, generally one each day. All canisters were later analysed for methane, CO, $CO_2$, NMHC ($C_2$–$C_8$) and some halocarbons at the laboratory in Jülich. The measurement techniques have been described by Rudolph et al. (1986).

The signal output of all instruments was stored on a personal computer for evaluation with a commercially available software package (Apex, Autochrome Inc., USA).

## 3. Results and discussion

### *3.1. Carbon monoxide*

Fig. 3 shows the time series of the mixing ratios of carbon monoxide measured with the in-situ technique. The original data set showed some outliers, which had always higher mixing ratios. Those have been removed, because they reflect interferences of local sources like skidoos, cars, or fossil fuel combustion from the village's generator station. This was confirmed by increased NMHC mixing ratios in samples collected simultaneously or by observations of cars or skidoos passing the measurement site. Included in Fig. 3 are the results from the analyses of the canister samples. It can be seen that on average both measurements agree very well, although the canister samples exhibit a somewhat larger scatter. The general trend of the CO mixing ratio is a continuous decrease from 140 ppb to 85 ppb. There are two reasons for this behaviour. During winter no photochemical decomposition occurs because of the complete darkness in arctic winter. Additionally, there is a low pressure system located over the north pole, which moves polluted air masses from Eastern Europe and Asia into the Arctic (Ottar, 1987; Barrie, 1986). After polar sunrise the low pressure system shifts in a way, that clean oceanic air masses from the North Pacific and Atlantic enter the Arctic. Furthermore, photochemistry starts due to OH radical production and becomes more important as the solar zenith angle decreases. Thus, the trend seen in Fig. 3 is part of the seasonal trend seen in the entire arctic for a variety of trace gases (Rudolph et al., 1996; Beine et al., 1996; Jobson et al., 1994; Solberg et al., 1996). The dashed line in Figure 3 represents the ozone mixing ratio at ground level, which was recorded at the airfield by the Institut für Umweltphysik, Heidelberg, Germany. It is obvious that there is no correlation between the CO and $O_3$ mixing ratios.

### *3.2. Hydrocarbon measurements*

*3.2.1. Comparability of the different methods of NMHC analyses.* Figs. 4a (ethyne) and b (propene)

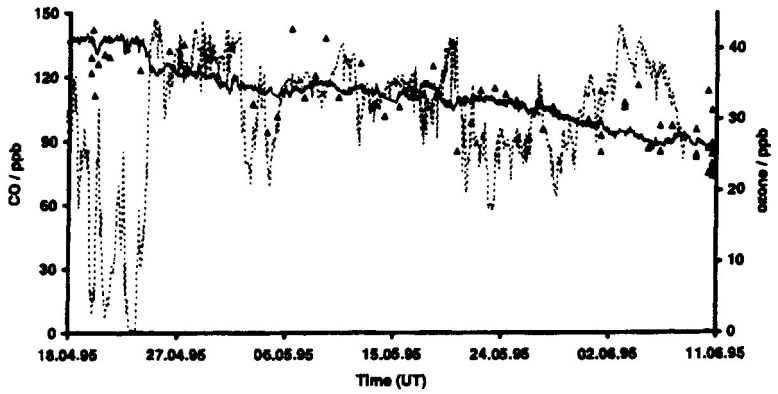


*Fig. 3.* Time series of carbon monoxide and ozone mixing ratios determined by different methods and at different locations. Solid line: in-situ measurements (Gruvebadet), solid triangles: canister samples (Zeppelin Mountain), open triangles: canister samples (Gruvebadet), dashed line: ozone (airport). Institut für Umweltphysik, Heidelberg, Germany (H. Lorenzen-Schmidt personal communication).

Table 3. *Comparability of the different methods of NMHC analysis*

| | GC 1/GC 2 | | | | | In-situ methods/canister sampling | | | | |
|---|---|---|---|---|---|---|---|---|---|---|
| | Percentile | | | $mr_{mean}$ | | Percentile | | | $mr_{mean}$ | |
| Compound | 25% | 50% | 75% | ppt | $N$ ($N_{tot}$) | 25% | 50% | 75% | ppt | $N$ ($N_{tot}$) |
| $C_2H_6$ | 0.98 | 1.02 | 1.03 | 1400 | 7 (7) | 0.95 | 0.99 | 1.02 | 1080 | 15 (15) |
| $C_2H_4$ | | 1.05 | | 20 | 1 (8) | 0.86 | 0.90 | 0.93 | 32 | 2 (5) |
| $C_2H_2$ | 0.94 | 1.05 | 1.15 | 200 | 37 (37) | 0.92 | 1.05 | 1.12 | 140 | 18 (20) |
| $C_3H_8$ | 0.83 | 0.98 | 1.34 | 200 | 9 (9) | 1.01 | 1.09 | 1.12 | 150 | 17 (17) |
| $C_3H_6$ | 1.04 | 1.15 | 1.48 | 11 | 3 (21) | 0.19 | 0.55 | 0.58 | 36 | 5 (14) |
| i-$C_4H_{10}$ | 1.02 | 1.15 | 1.25 | 14 | 14 (36) | 0.97 | 0.97 | 0.97 | 11 | 1 (4) |
| n-$C_4H_{10}$ | 1.33 | 1.49 | 1.64 | 26 | 32 (33) | 1.11 | 1.38 | 1.52 | 16 | 10 (20) |
| i-$C_5H_{12}$ | | 1.11 | | 5 | 1 (20) | | | | | 0 (12) |
| n-$C_5H_{12}$ | 0.88 | 1.03 | 1.10 | 4 | 4 (27) | | | | | 0 (15) |
| $C_6H_6$ | | | | | | 0.93 | 1.00 | 1.28 | 40 | 13 (14) |
| $CH_3Cl$ | | | | | | 0.92 | 0.99 | 1.01 | 490 | 14 (14) |

The comparison could not be carried out for alkanes $>C_5$ and aromatics $>C_7$ since all simultaneous measurements were below the detection limit. $N$: number of simultaneous measurements above detection limit, $N_{tot}$: total number of simultaneous measurements.

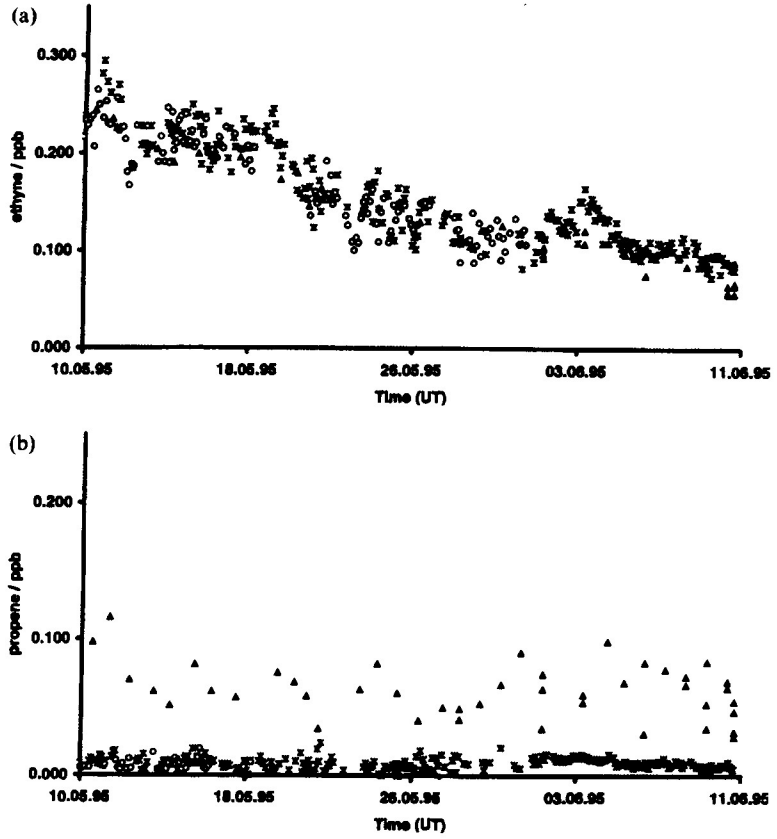


*Fig. 4.* (a,b) Comparison of the ethyne and propene mixing ratios determined by different methods and at different locations. Stars: GC1 in-situ measurements (Gruvebadet), circles: GC2 in-situ measurements (Gruvebadet), solid triangles: canister samples (Zeppelin Mountain), open triangles: canister samples (Gruvebadet).

show time series recorded by the different methods between 10 May and 9 June. The plots show a very good agreement between the two in-situ methods. For ethyne also the in-situ and the canister measurements agree. The sampling intervals of the two in-situ methods overlapped for 37 pairs of measurements. The median ratio of the results of both methods was 1.05 at a mean mixing ratio of 200 ppt. Thus, no significant deviations between the two methods were found.

This holds for most of the determined substances (Table 3). It should be noted that the air samples compared here were not identical, but could differ by as much as 25 min in their mean sampling time (total sampling interval 50–60 min). The difference of n-butane mixing ratios determined by the two in-situ methods is somewhat higher than what would be expected from the errors estimated for the methods. In 31 of 33 data pairs for n-butane the mixing ratio determined with GC1 was higher than the one determined with GC2 (mean difference between the methods 9 ppt). A possible reason for this behaviour might be the broad n-butane peak recorded with GC2,

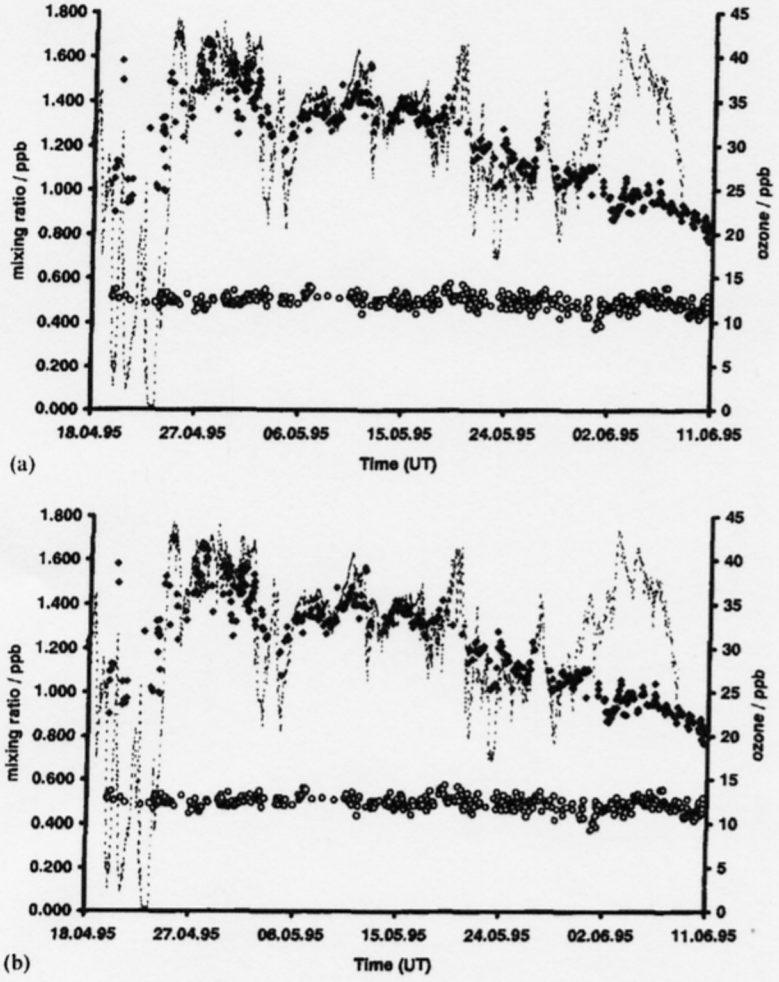


*Fig. 5.* Time series of several VOC and ozone mixing ratios. Marks on time axis were set to mid-night. Dashed line: ozone (airport). (a) diamonds: ethane, open circles: chloromethane; (b) diamonds: ethyne, open circles: propane; (c) diamonds: n-butane, open circles: i-butane, crosses: benzene; (d) squares: methane.

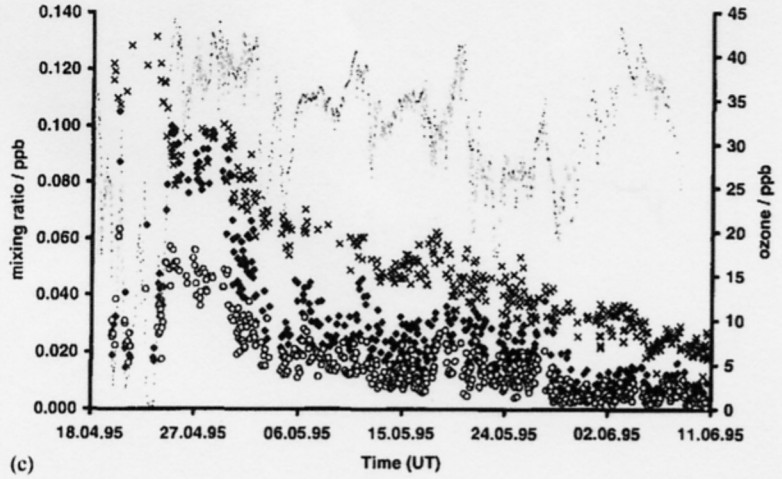


(c)

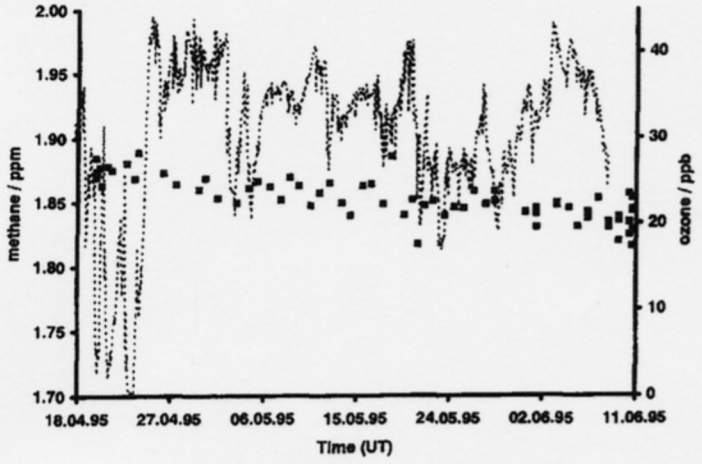


(d)

*Fig. 5* (cont'd).

which may result in an inadequate baseline definition.

For propene, only the two in-situ methods are in good agreement, (21 pairs, 18 below detection limit, mean difference 4 ppt at a mean mixing ratio of 11 ppt), the canister samples differ. Their mixing ratio is always higher. We believe, that, although we condition our canisters carefully prior to sampling, some propene is formed at the canisters' inner surface. Systematic errors of the in-situ analysis are very unlikely, since we observed no significant deviations between the carbon response for alkenes and alkanes when analysing calibration gas mixtures. A destruction of alkenes by reaction with atmospheric ozone during the preconcentration of the air sample can be ruled out, because the difference between the canister and in-situ results were found during the major ozone depletion period, too. Koppmann et al. (1995), who were using an identical preconcentration system, showed that ozone mixing ratios up to 100 ppb had no effect on the determination of alkene mixing ratios. The good comparability (except for propene in canisters) of the different NMHC measurement techniques emphasises the quality of the data collected during the entire campaign. Since most of the canister samples were collected on Zeppelin Mountain whereas in-situ measurements were carried out at sea level, it seems, that there is no significant difference between the two sites.

A comparison between samples from the "Gruvebadet" and Zeppelin Mountain having overlapping sampling intervals shows that the variation is statistical within the error limits of the methods. This gives a lower limit for the height of the well mixed boundary layer and the vertical extension of the changes of the NMHC pattern during ozone depletion events.

For the further analyses of the hydrocarbon data the data sets recorded with the different methods were combined. In addition to the propene data from the canister samples the i-butane and i-pentane canister data were excluded from that combination, because of an incomplete chromatographic separation, which resulted in large experimental errors.

*3.2.2. Hydrocarbon time series.* Time series of the most abundant NMHC and methane are plotted together with ozone in Fig. 5. Measurements started during the only major ozone depletion event (18–24 April). A second period of lower ozone mixing ratios was encountered between 2–5 May. An enlarged view of the major ozone depletion period (18–24 April) is given in Fig. 6 for the same set of substances.

Apart from the changes observed during the ozone depletion events the general trend is a

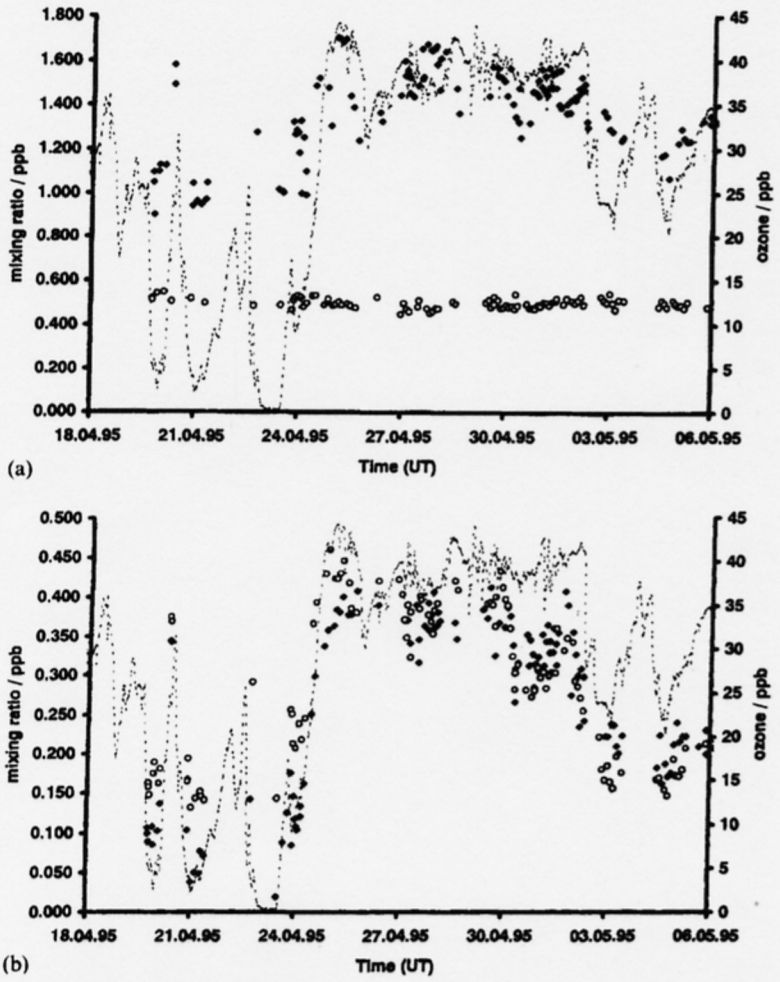


*Fig. 6.* (a–c) VOC and ozone mixing ratios during ozone depletion periods. Marks on time axis were set to midnight. Dashed line: ozone (airport). Symbols have the same meaning as in Fig. 5.

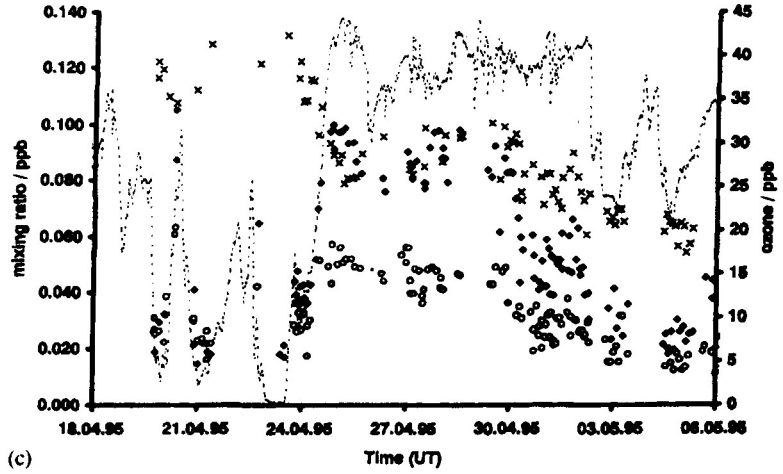


*Fig. 6* (cont'd).

decrease in mixing ratios for most substances between mid of April and early June (Fig. 5). Only chloromethane remains almost constant during the measurements. Its atmospheric lifetime against OH is in the order of 9 month, which is long enough to generate a uniform distribution in the northern hemisphere. Thus, in the case of chloromethane there is no dilution by air masses of oceanic origin entering the arctic. The enlarged view of the major depletion episode shows that the measured compounds can be grouped in two classes. The first (benzene, chloromethane, CO, and methane) shows no correlation with the ozone mixing ratio, whereas the second (alkanes and ethyne) does.

*3.2.3. Correlation between NMHC and ozone.* Fig. 7 show correlation plots of ozone and some of the NMHC. Linear regressions were plotted for the two ozone depletion periods (18–24 April, 2–5 May). Table 4 summarizes the regression data.

In general, the positive correlation between NMHC and ozone is reasonable for light alkanes and ethyne for the major ozone depletion event ($r^2=0.54$ (ethane) $-0.90$ (propane)). Weaker correlations ($r^2=0.5$) are found for i-butane and the pentanes and no positive correlation was found for benzene, chloromethane, propene, and ethene. The correlation coefficients for the less intense ozone depletion period between 2–5 May are generally lower than those found for the first depletion period. Coefficients vary between 0.36 for i-butane and 0.72 for propane. The pentane, ethene, propene, and benzene mixing ratios do not show any significant correlation with ozone during this period. The negative correlation coefficients calculated for benzene versus ozone and CO versus ozone are due to the decreasing mixing ratios of the organic trace gases together with the 'recovery' of ozone at the end of the event. The lack of correlation between alkenes and ozone has also been observed by other groups (Kieser et al., 1993; Jobson et al., 1994; Solberg et al., 1996; Hopper et al., 1994). The reason might be the small mixing ratios which at least for propene are too close to the detection limit, so that small fluctuations and experimental errors (canister sampling was used in all of the studies cited) could easily mask a possible correlation.

The reactivity data in Table 5 can be used to explain the correlation of ozone with alkanes/ethyne and the absence of correlations with benzene, CO, chloromethane, and methane. The reactivity towards chlorine atoms differs substantially between the two groups of compounds (see Table 5). Whereas the rates of reaction for CO and $CH_3Cl$ with Cl atoms or OH radicals do not differ substantially the reaction of Cl with alkanes or ethyne is a factor of 50 to 350 faster than with OH.

To estimate the changes in NMHC mixing ratios that would be observed under the presence of chlorine radicals the 3 day measurement period (14.-16.5.95) was chosen as a reference. During

this period the ozone mixing ratio was nearly constant and no local pollution interfered. The expected change of the mixing ratios resulting from the reactions with Cl-atoms can be calculated by:

$$[HC]_{depl.} = [HC]_{initial} \exp(-k_{HC,Cl} \int [Cl]/dt), \quad (1)$$

with

$[HC]_{depl./initial}$: hydrocarbon concentration during depletion (Cl chemistry)/initially

$k_{HC,Cl}$: rate constant for the reaction between hydrocarbon and Cl

$\int [Cl]dt$: time integral of the Cl concentration

The mean mixing ratios of each compound (Table 6, column 2) were used as $[HC]_{initial}$, $dt$ was set to 3 days and the chlorine concentration was assumed to be $10^3$, $10^4$, and $10^5$ cm$^{-3}$, respectively. Table 6 summarizes the changes expected for different Cl atom concentrations for some hydrocarbons, CO, and chloromethane. It is obvious that changes in mixing ratios due to free chlorine atoms will not be observable by monitoring compounds of the first group like methane, CO, chloromethane, and benzene unless Cl atom concentrations of $10^5$ cm$^{-3}$ are exceeded. Otherwise, the expected changes are below the experimental errors. Alkanes and ethyne mixing ratios will be substantially effected by chlorine radical induced decomposition, if the radical concentration exceeds about $10^4$ cm$^{-3}$. In this case halogen induced changes are distinguishable from background variations and experimental errors. The use of heavier alkanes is somewhat limited, because of their higher relative variability.

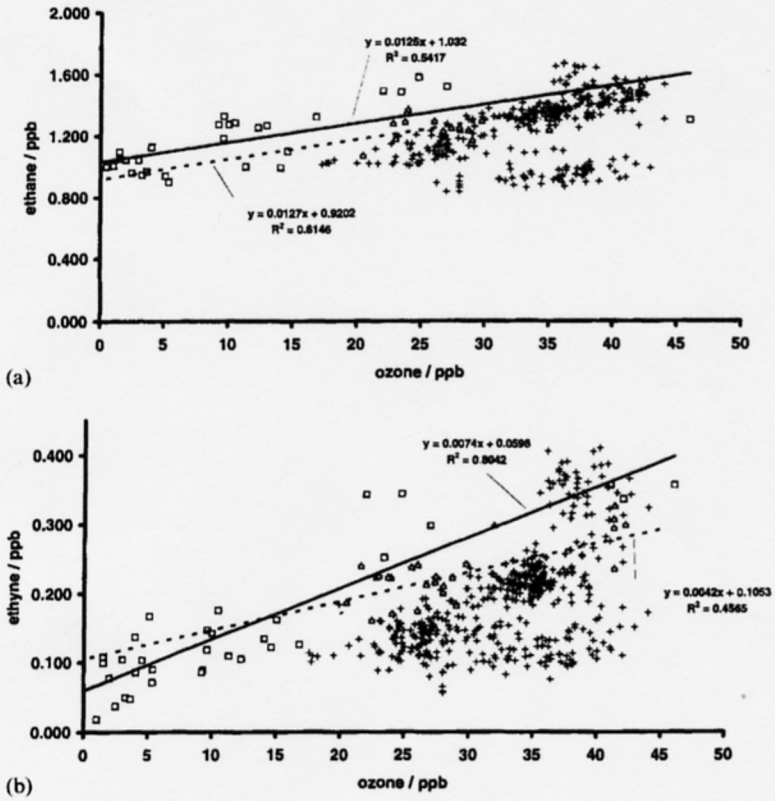


*Fig. 7.* (a–d) Plots of ozone versus selected NMHC including linear correlations. triangles, dashed line: minor depletion period (2 May 00:00–5 May 23:59), squares, solid line: major ozone depletion period (18 April 00:00–24 April 23:59), crosses: normal ozone.

The observation that compounds like benzene and CO show no change in their mixing ratios during the ozone depletion event supports the idea that changes in meteorology cannot explain the phenomenon of ozone depletions. A chemical explanation based on halogen atoms seems much more likely and is able to account for the observed changes in NMHC pattern.

*3.2.4. Correlation among hydrocarbons.* Another way to look at the changes in NMHC pattern during an ozone depletion period is to plot the mixing ratios of two hydrocarbons against each other. Certain pairs have been used as evidence that halogen atoms are involved in the depletion chemistry (Jobson et al., 1994; Solberg et al., 1996). The compounds to be chosen should have similar rate constants for reaction with OH radicals and very different rate constants for reactions with Cl radicals. From Table 5 these pairs are easy to find. Propane and benzene, trichloroethene and i-butane, n-butane and i-butane, and n-hexane and toluene as well as toluene and n-heptane would be such pairs. The assumption that the NMHC pattern in the original air masses are identical is justified by the absence of changes in the methane, CO, benzene, and PAN (Müller, personal comunication) mixing ratios.

The problem that arises with the favourable pairs named above is that n-hexane, n-heptane, and toluene were only present at mixing ratios $< 10$ ppt, which are close to the detection limit of the methods used. Additionally, local pollution due to exhausts and evaporation of fossil fuels was more pronounced for hydrocarbons $> C_4$ (except benzene). Thus, we only could make use of the plots of propane versus benzene and i-butane/n-butane versus n-butane (Fig. 8). The data recorded during the major ozone depletion generally do not fit into the overall trend. The

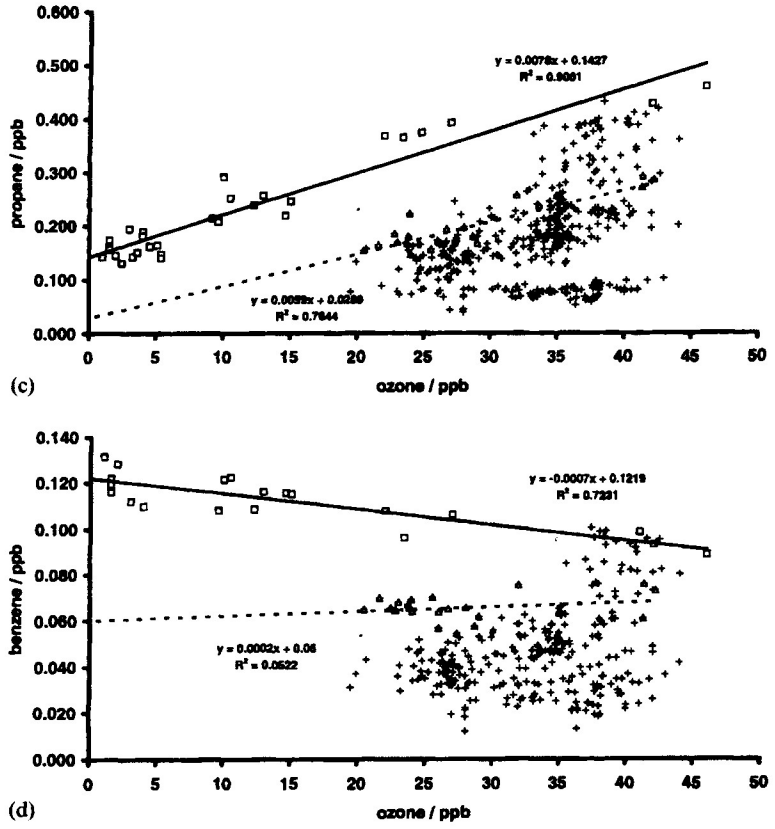


*Fig. 7* (cont'd).

Table 4. *Regression coefficients ($r^2$) for linear regressions of ozone versus hydrocarbons for the two ozone depletion periods (18 April 00:00–24 April 23:59, 2 May 00:00–5 May 23:59) and the whole campaign, negative correlations are marked (-)*

| Compound | 18–24 April Regression coefficient | 2–5 May Regression coefficient | Whole campaign Regression coefficient |
|---|---|---|---|
| CO | 0.158 (-) | 0.058 | 0.164 (-) |
| $CH_3Cl$ | 0.023 (-) | 0.002 | 0.002 |
| $CH_4$ | 0.045 (-) | 0.014 | 0.267 (-) |
| $C_6H_6$ | 0.723 (-) | 0.052 | 0.056 |
| $C_2H_6$ | 0.542 | 0.615 | 0.176 |
| $C_2H_4$ | 0.065 (-) | 0.097 | 0.013 |
| $C_2H_2$ | 0.804 | 0.457 | 0.286 |
| $C_3H_8$ | 0.900 | 0.750 | 0.086 |
| $C_3H_6$ | 0.015 (-) | 0.082 | 0.050 (-) |
| i-$C_4H_{10}$ | 0.517 | 0.363 | 0.008 |
| n-$C_4H_{10}$ | 0.817 | 0.516 | 0.075 |
| i-$C_5H_{12}$ | 0.475 | 0.160 | 0.048 |
| n-$C_5H_{12}$ | 0.530 | 0.056 | 0.025 |
| n-$C_6H_{14}$ | 0.131 | 0.024 | 0.001 |
| n-$C_7H_{16}$ | 0.020 | 0.014 | 0.018 |
| $C_7H_8$ | 0.026 | 0.000 | 0.012 |

Table 5. *Rate constants for the reaction VOC + Cl/Br → products*

| Compound | $k$ (OH)/cm$^3$ s$^{-1}$ | $k$ (Cl)/cm$^3$ s$^{-1}$ | $k$ (Br)/cm$^3$ s$^{-1}$ | $k$ (Cl)/$k$ (OH) | $k$ (Br)/$k$ (OH) |
|---|---|---|---|---|---|
| CO | $1.44\cdot10^{-13}$ (a[4]) | $3.15\cdot10^{-14}$ (a[6]) | | 0.2 | |
| $CH_3Cl$ | $2.16\cdot10^{-14}$ (b[1]) | $3.60\cdot10^{-14}$ (a[5]) | | 1.7 | |
| $CH_4$ | $2.07\cdot10^{-15}$ (b[1]) | $4.33\cdot10^{-14}$ (b[1]) | | 20.9 | |
| $C_6H_6$ | $9.11\cdot10^{-13}$ (b[2]) | $1.50\cdot10^{-11}$ (a[7]) | | 16.5 | |
| $C_2H_6$ | $1.57\cdot10^{-13}$ (b[1]) | $5.37\cdot10^{-11}$ (b[6]) | | 342.6 | |
| $C_2H_4$ | $1.11\cdot10^{-11}$ (b[2]) | $9.29\cdot10^{-11}$ (a[8]) | $1.60\cdot10^{-13}$ (a[11]) | 8.4 | 0.01 |
| $C_2H_2$ | $6.66\cdot10^{-13}$ (b[2]) | $6.94\cdot10^{-11}$ (b[6]) | $1.54\cdot10^{-13}$ (b[11]) | 104.2 | 0.23 |
| $C_3H_8$ | $7.56\cdot10^{-13}$ (b[1]) | $1.41\cdot10^{-10}$ (b[6]) | | 157.7 | |
| $C_3H_6$ | $3.00\cdot10^{-11}$ (b[3]) | $3.22\cdot10^{-10}$ (a[8]) | $2.70\cdot10^{-12}$ (a[6]) | 70.7 | 0.09 |
| i-$C_4H_{10}$ | $2.03\cdot10^{-12}$ (b[2]) | $1.51\cdot10^{-10}$ (a[8]) | | 74.4 | |
| n-$C_4H_{10}$ | $2.18\cdot10^{-12}$ (b[2]) | $1.97\cdot10^{-10}$ (a[7]) | | 90.4 | |
| i-$C_5H_{12}$ | $3.90\cdot10^{-12}$ (a[2]) | $2.02\cdot10^{-10}$ (a[7]) | | 51.9 | |
| n-$C_5H_{12}$ | $4.05\cdot10^{-12}$ (b[2]) | $2.02\cdot10^{-10}$ (a[7]) | | 50.0 | |
| n-$C_6H_{14}$ | $5.57\cdot10^{-12}$ (a[2]) | $3.02\cdot10^{-10}$ (a[7]) | | 54.2 | |
| n-$C_7H_{16}$ | $7.20\cdot10^{-12}$ (a[2]) | $3.40\cdot10^{-10}$ (a[7]) | | 47.2 | |
| $C_7H_8$ | $7.58\cdot10^{-12}$ (b[2]) | $5.89\cdot10^{-11}$ (a[7]) | | 7.7 | |
| $C_2HCl_3$ | $2.96\cdot10^{-12}$ (b[3]) | $8.08\cdot10^{-11}$ (a[12]) | | 27.2 | |
| $C_2Cl_4$ | $7.72\cdot10^{-14}$ (b[2]) | $4.61\cdot10^{-11}$ (b[10]) | | 596.0 | |
| $O_3$ | $3.10\cdot10^{-14}$ (b[2]) | $9.55\cdot10^{-12}$ (b[9]) | $6.72\cdot10^{-13}$ (b[9]) | 308.1 | 21.7 |

Preferably, the data tabulated for 250K should be used, since this temperature was encountered during low ozone periods. Data for 298K is listed in cases where the temperature dependence of the rate constant is unknown. The values are those recommended by NIST or JPL Publication 94–26 (a: 298 K, b: 250 K).

1: Atkinson et al. (1992)
2: Atkinson (1986)
3: Atkinson et al. (1989)
4: Greenblatt et al. (1982)
5: Taylor et al. (1993)
6: DeMore (1994)
7: Atkinson et al. (1985)
8: Wallington et al. (1988)
9: Nicovich et al. (1990)
10: Nicovich et al. (1996)
11: Barnes et al. (1993)
12: Atkinson et al. (1987)

Table 6. *Mean mixing ratios and relative standard deviations for a 3 day measurement period (14.-16.5.95) and changes that would be induced by three different Cl atom concentrations after 3 days ([OH] = 0 cm$^{-3}$)*

| Measurements (14.-16.5.95) | | | Calculated deviation from mean/% | | |
|---|---|---|---|---|---|
| Compound | Mean/ppb | rsd/% | [Cl] = $10^3$ cm$^{-3}$ | [Cl] = $10^4$ cm$^{-3}$ | [Cl] = $10^5$ cm$^{-3}$ |
| CO | 110.95 | 1.44 | 0.00 | 0.01 | 0.08 |
| $CH_3Cl$ | 0.488 | 4.27 | 0.00 | 0.01 | 0.09 |
| $CH_4$ | 1.855 | 0.73 | 0.00 | 0.01 | 0.11 |
| $C_6H_6$ | 0.049 | 6.98 | 0.39 | 3.81 | 32.21 |
| $C_2H_6$ | 1.350 | 2.80 | 1.38 | 12.99 | 75.14 |
| $C_2H_4$ | 0.030 | 27.91 | 2.38 | 21.40 | 91.00 |
| $C_2H_2$ | 0.215 | 7.96 | 1.78 | 16.46 | 83.45 |
| $C_3H_8$ | 0.177 | 6.28 | 3.04 | 26.54 | 95.42 |
| $C_3H_6$ | 0.011 | 68.80 | 8.01 | 56.60 | 99.98 |
| i-$C_4H_{10}$ | 0.011 | 32.85 | 3.84 | 32.37 | 98.00 |
| n-$C_4H_{10}$ | 0.021 | 26.95 | 5.60 | 43.79 | 99.68 |
| $O_3$ | 34.80 | 3.51 | 0.25 | 2.44 | 21.93 |

i-butane/n-butane data for the minor depletion episode lie mostly within the scatter of the data for "normal ozone", whereas the propane/benzene ratio differs significantly from the non-depletion data. This behaviour is due to the higher sensitivity of the propane/benzene ratio towards Cl chemistry. This strongly supports the concept that chlorine radicals were involved in the chemistry taking place during those periods.

The mean value of the i-butane/n-butane ratio (non-depletion) plotted in Fig. 8b is $0.55 \pm 0.01$ (mean $\pm$ deviation of the mean), which is in good agreement with published data. Other groups reported ratios of 0.52 for the free troposphere (Penkett et al., 1993) and 0.52 (Solberg et al., 1996) as well as 0.53 (Jobson et al., 1994) in the arctic boundary layer.

*3.2.5. Estimate of time-integrated halogen concentrations.* From the change in hydrocarbon patterns during ozone depletion events, it is possible to calculate time-integrated halogen atom concentrations. The basic assumption is that the difference between "non-depletion" and "depletion event" NMHC concentrations are caused by halogen atom reactions. Rearrangement of equation 1 yields an expression from which the time integrated chlorine atom concentration can be calculated.

$$-\int [\mathrm{Cl}]\,dt = \frac{1}{k_{\mathrm{HC,Cl}}} \ln \frac{[\mathrm{HC}]_{\mathrm{depl.}}}{[\mathrm{HC}]_{\mathrm{initial}}}. \quad (2)$$

Since $[\mathrm{HC}]_{\mathrm{depl.}}$ was measured and $k_{\mathrm{HC,Cl}}$ is known from literature (Table 5), the central question is: What are the NMHC mixing ratios ($[\mathrm{HC}]_{\mathrm{initial}}$) in an ozone depleted air mass if there is no effect from chlorine radicals. The difficulty is that an ozone depletion event always means a change in the air mass at the measuring site. However, since the arctic boundary layer seems to be quite well mixed, it can be assumed as a first approximation that an interpolation between the NMHC mixing ratios before and after the ozone depletion event is a measure for $[\mathrm{HC}]_{\mathrm{initial}}$. This assumption is supported by the mixing ratios of benzene, carbon monoxide, methane, and PAN, which do not show any significant changes that could be correlated with low ozone events. Unfortunately NMHC measurements just started during the only major ozone depletion period, thus an extrapolation of the NMHC trend is needed to calculate $[\mathrm{HC}]_{\mathrm{initial}}$. To improve the accuracy of the NMHC trend the data presented here were combined with unpublished hydrocarbon data by N. Schmidbauer and S. Solberg (Norwegian Institute for Air Research (NILU), Kjeller, Norway). The data cover the time period between 1 April 1995 and 26 May 1995 and resulted from daily canister sampling on Zeppelin Mountain. The data compare quite well with this study, except for benzene and ethyne, where NILU's data are a factor of 1.39 and 1.22 higher than the data presented here. Details are given by

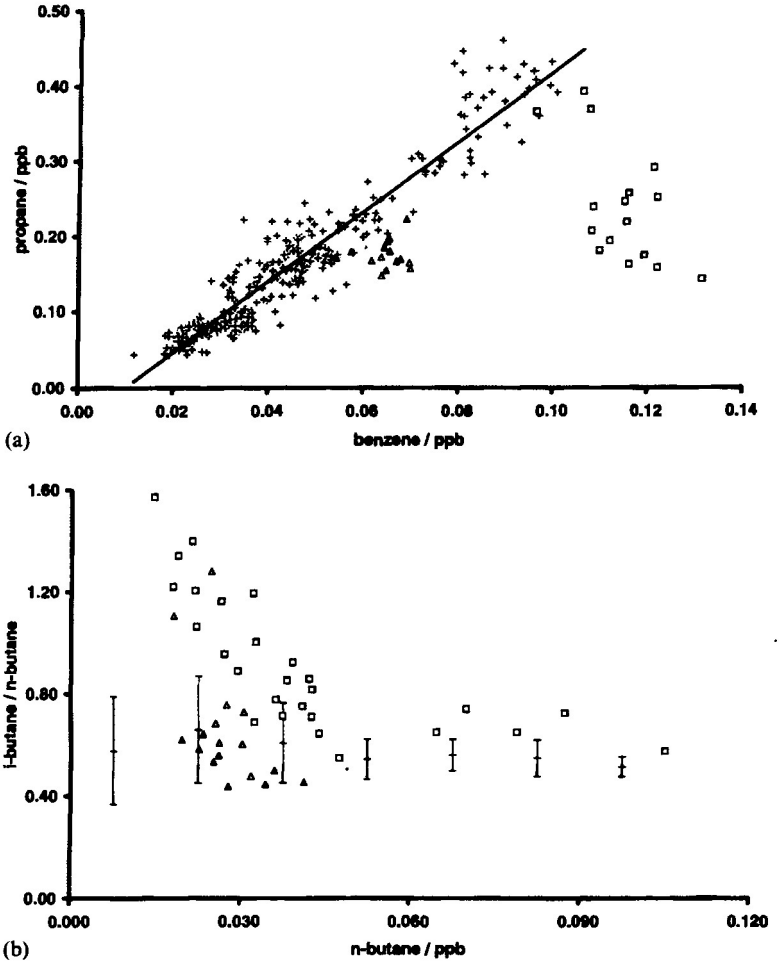


*Fig. 8.* (a,b) Plots of propane versus benzene and the i-butane/n-butane ratio versus n-butane. crosses: ozone >30 ppb (plot 8b mean value±standard deviation for 0.015 ppb intervals of n-butane mixing ratio), triangles: minor depletion period (2–5 May, ozone <30 ppb), squares: major depletion period (18–24 April, ozone <30 ppb).

Ramacher (1997). The NILU data were corrected for the difference between the two data sets and combined with the results of this study.

Examples of such estimates of background NMHC mixing ratios are given in Fig. 9a–b for ethane and n-butane. The fits were calculated according to the least-square method for hydrocarbon data recorded at ozone mixing ratios exceeding 30 ppb. The plots indicate that the best agreement between measured and calculated hydrocarbon concentrations was achieved by using different type of fits for interpolation of the background mixing ratios of different hydrocarbons. Thus, a linear fit was used for ethane and exponential fits were used for ethyne propane and the butanes. However, in the case of n-butane a single interpolation is not sufficient. When focusing on ozone depletions separate fits for the two ozone depletion periods should be used. For the major ozone event the interpolation of FZJ and NILU data until day 30 fits the measurements best, whereas for the minor depletion an exponential fit to the whole data seems to be the best description for the observed mixing ratios.

The effect of Br-atoms can be derived from the depletion of ethyne. Ethyne is one of the few

compounds which react fast enough with bromine atoms to see a significant effect on its mixing ratio. In order to obtain the time-integrated bromine atom concentration, the effect of the time integrated Cl concentration (calculated from the depletion in ethane and propane) for ethyne was calculated. The corrected ethyne mixing ratio was then treated as $[C_2H_2]_{initial}$ and $\int[Br]dt$ was calculated from an equation equivalent to eq. (2). Table 7 presents the results of the calculation of the time integrated halogen atom concentrations encountered during the ozone depletion periods 18–24 April 1995 and 2–5 May 1995. For the first episode, the calculated time integrated Cl and Br atom concentrations are in the range of $10^{10}$ and $10^{13}$ s cm$^{-3}$, respectively. Assuming that each halogen atom causes a net ozone loss these numbers translate to a chlorine induced ozone change of about 8% and a bromine induced ozone change of about 100%. The total ozone change is dominated by the loss through bromine radicals and amounts to almost 100%, which explains the observed ozone losses (>95%) quantitatively. The calculated concentrations of Br and Cl atoms compare well to values estimated by other groups (Jobson et al., 1994; Solberg et al., 1996).

However, for the second depletion event our simple picture is not able to explain the ozone loss quantitatively. The concentrations of halogen atoms calculated for that period are about $3–5 \cdot 10^9$ s cm$^{-3}$ for chlorine and about $1–2 \cdot 10^{12}$ s cm$^{-3}$ for bromine. This would yield ozone losses between 50–70%, whereas only losses of 25–40% were observed. The errors of the calculated time integrated halogen atom concentrations together with the uncertainty of the total ozone losses are tabulated in Table 8. They depend on the statistical error of the NMHC measurements, the accuracy of the interpolation to calculate $[HC]_{initial}$, and the uncertainty of the rate constants used. The analysis shows that the errors of the calculated time integrated radical concentrations varied between $0.3–1.2 \cdot 10^9$ s cm$^{-3}$ for chlorine and $1–5 \cdot 10^{12}$ s cm$^{-3}$ for bromine. The error of the calculated ozone change for major ozone depletions is in the order of less than 1%, whereas for minor depletions it increases to 25–40%. Thus, even for minor depletions, the deviations between observed and calculated change of the ozone mixing ratio are within the reported error limits. However, there seems to be a systematic overestimation of the halogen induced ozone change, which becomes more obvious for minor ozone depletion events. This might be due to the assumption that each halogen atom calculated from the change in hydrocarbon mixing ratios yields a net

Table 7. *Estimate of the time integrated halogen atom concentration during the ozone depletion periods*

| | $-\int[X\cdot]dt/10^9$ s cm$^{-3}$ | | | $O_3$ change/% | | | |
|---|---|---|---|---|---|---|---|
| Episode | X=Cl ($C_2H_6$) | X=Cl ($C_3H_8$) | X=Br ($C_2H_2$) | Cl· ind. | Br· ind. | Total | Observed |
| 21 April | 9.8 | 8.4 | 9860 | 8.1 | 99.9 | 99.9 | 95.0 |
| 23 April | 8.4 | 7.8 | 16000 | 7.7 | 100.0 | 100.0 | 99.0 |
| 3 May | 2.7 | 2.8 | 955 | 2.8 | 47.6 | 49.1 | 23.5 |
| 5 May | 4.8 | 3.9 | 1720 | 3.5 | 68.7 | 69.8 | 38.0 |

Table 8. *Errors of the time-integrated halogen atom concentrations and the calculated change of the ozone mixing ratio*

| | $\Delta\int[X\cdot]dt/10^9$ s cm$^{-3}$ | | Error of the calculated ozone change/% |
|---|---|---|---|
| Episode | X=Cl | X=Br | Cl+Br effect |
| 21 April 95 | 0.9 | 3880 | 0.30 |
| 23 April 95 | 0.5 | 5090 | 0.01 |
| 3 May 95 | 0.4 | 1250 | 43.15 |
| 4 May 95 | 1.2 | 1240 | 25.31 |

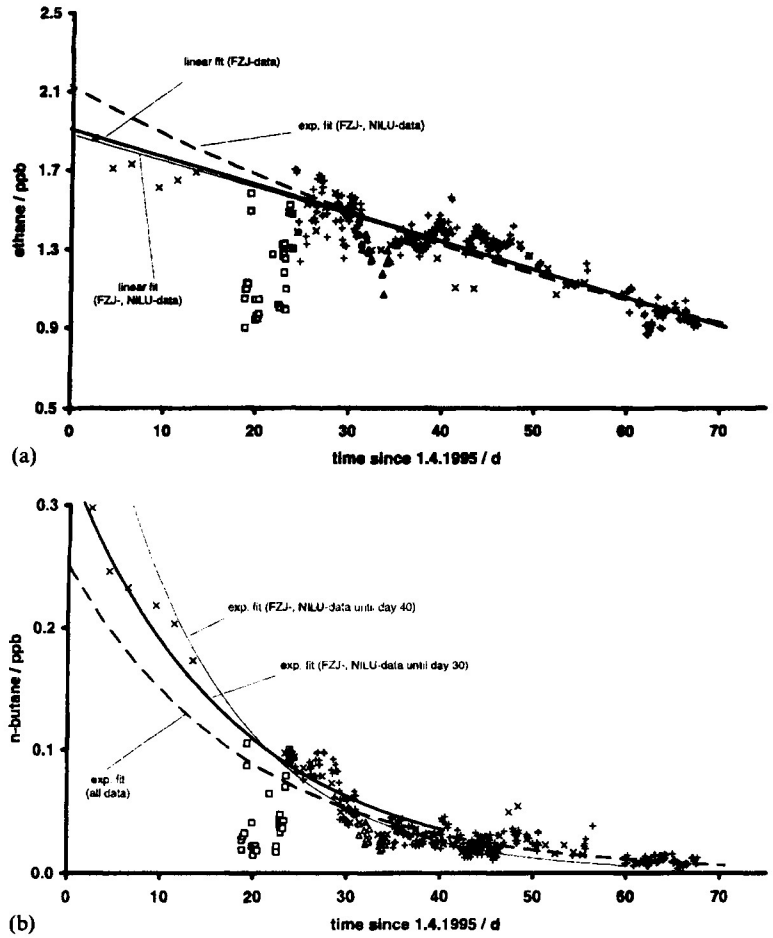


*Fig. 9.* (a,b) Fitting curves of the seasonal decrease of ethane and n-butane mixing ratios. Crosses: ozone >30 ppb, ×: NILU canister data, triangles: minor depletion period (2–5 May, ozone <30 ppb), squares: major depletion period (18–24 April, ozone <30 ppb), only the non-depletion data were fitted.

ozone destruction. There are some reaction pathways for which this is not the case. An example for an reaction pathway which has to be considered is:

$$BrO + ClO \rightarrow Br + ClO_2$$

$$ClO_2 + h\nu \rightarrow ClO + O\ (^3P)$$

$$O\ (^3P) + O_2 \rightarrow O_3$$

This reaction pathway recycles bromine oxide to bromine atoms but also generates ozone. To account for reaction like this when estimating the ozone changes a detailed model calculation, which is beyond the scope of this paper, would be needed.

The good time resolution of the NMHC data allows the calculation of a time series of the time integrated halogen atom concentration. To do so, the NMHC data for "normal ozone" is fitted by trend curves as described above (Fig. 9). Fig. 10 shows the calculated integrated chlorine and bromine concentrations along with ozone data. The correlation between the calculated radical concentrations and the ozone mixing ratio is obvious. For normal ozone levels the mean values of $\int[Br]dt$ and $\int[Cl]dt$ were found to be $6 \cdot 10^{10}$ s cm$^{-3}$ (standard deviation of mean $4 \cdot 10^{10}$ s cm$^{-3}$) and $-1.2 \cdot 10^{8}$ s cm$^{-3}$ (standard deviation of mean $5 \cdot 10^{7}$ s cm$^{-3}$), respectively. Thus, the

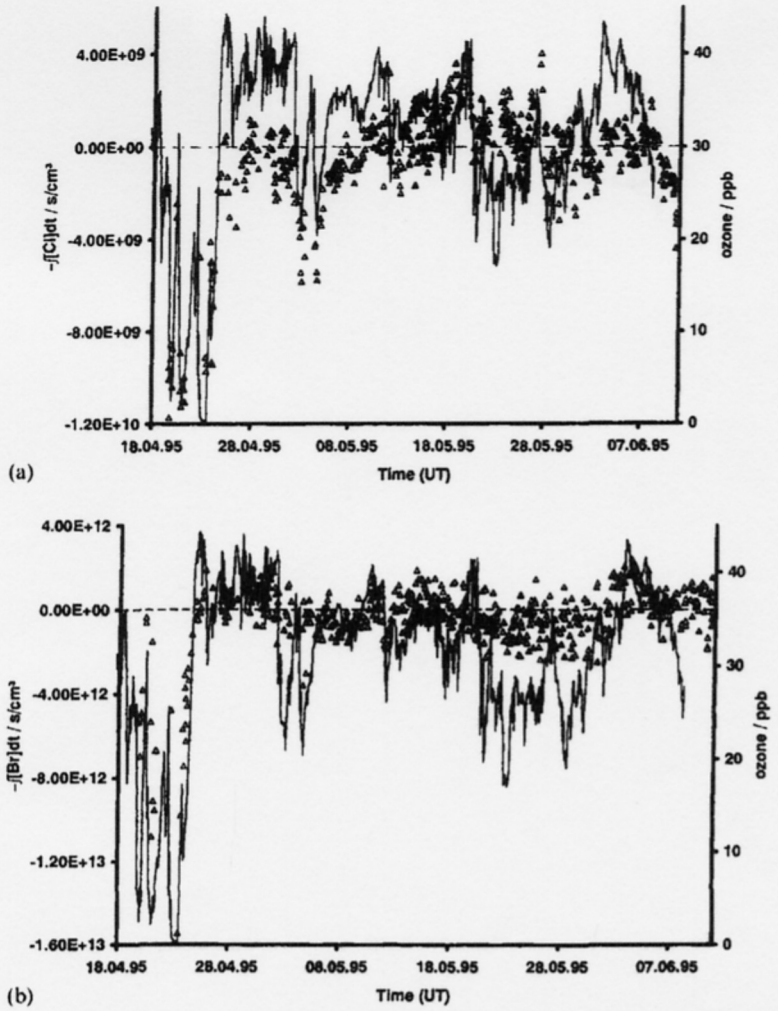


*Fig. 10.* (a,b) Plots of time integrated halogen atom concentrations. Triangles: time integrated halogen atom concentrations, solid line: ozone mixing ratio. The negative time integrated halogen atom concentrations were plotted to emphasise their correlation to ozone mixing ratios.

calculated time integrated radical concentrations for ozone depletions differ significantly from the background calculated for non-depletion periods.

## 4. Summary and conclusions

The observed changes in the NMHC mixing ratios during low ozone events strongly suggest the existence of high concentrations of halogen atoms during that period. A simple transport phenomenon is very unlikely to explain the observed changes in NMHC pattern and the ozone depletion. Based on this we can calculate time-integrated halogen atom concentrations which can account for the ozone depletion quantitatively. According to that calculation ozone is mainly depleted due to bromine atom induced chemistry, whereas Cl plays a minor rôle in ozone destruction. However, Cl is the main cause for the concurrent NMHC depletion.

A minor ozone depletion event was also attributed to halogen atom influence. However, from this simple calculation it is not possible to explain

the less intense event as precisely. Currently, there still seems to be a lack of understanding of the mechanism of ozone and NMHC depletion in the arctic troposphere.

## REFERENCES


Anlauf, K. G., Mickle, R. E. and Trivett, N. B. A. 1994. Measurement of ozone during Polar Sunrise Experiment 1992. *J. Geophys. Res.* **99**, 25345–25353.

Atkinson, R. and Aschmann, S. M. 1985. Kinetics of the gas-phase reactions of Cl atoms with chloroethenes at 296±2K and atmospheric pressure. *Int. J. Chem. Kinet.* **17**, 33–41.

Atkinson, R. 1986. Kinetics and mechanisms of the gas-phase reactions of the hydroxyl radical with organic compounds under atmospheric conditions. *Chem. Rev.* **86**, 69–77.

Atkinson, R. and Aschmann, S. M. 1987. Kinetics of the gas-phase reactions of Cl atoms with chloroethenes at 298±2K and atmospheric pressure. *Int. J. Chem. Kinet.* **19**, 1097–1109.

Atkinson, R., Baulach, D. L., Cox, R. A., Hampson, R. F., Kerr, J. A. and Troe, J. 1989. Evaluated kinetic and photochemical data for atmospheric chemistry, Supplement III. *J. Phys. Chem. Ref. Data* **18**, 881–1238.

Atkinson, R., Baulach, D. L., Cox, R. A., Hampson, R. F., Kerr, J. A. and Troe, J. 1992. Evaluated kinetic and photochemical data for atmospheric chemistry, Supplement IV. *J. Phys. Chem. Ref. Data* **21**, 1125–1568.

Barnes, I. Becker, K. H. and Overrath R. D. 1993. Oxidation of organic sulphur compounds. In: Tropospheric chemistry of ozone in polar regions (ed. Niki, H., Becker, K. H.). NATO ASI Ser., subseries I, *Global environmental change*, Springer Verlag, New York.

Barrie, L. A. 1986. Arctic air chemistry: an overview. In: *Arctic air pollution* (ed. B. Stonehouse). Cambridge University Press, Cambridge, London, New York, New Rochelle, Melbourne, Sydney, pp. 5–23.

Barrie, L. A., Bottenheim, J. W., Schnell, R. C., Crutzen, P. J. and Rasmussen R. A. 1988. Ozone destruction and photochemical reactions at polar sunrise in the lower Arctic atmosphere. *Nature* **334**, 134–141.

Beine, H.J, Jaffe, D. A., Blake, D. R., Atlas, E. and Harris, J. 1996. Measurements of PAN, alkyl nitrates, ozone, and hydrocarbons during spring in interior Alaska. *J. Geophys. Res* **101**, 12613–12619.

Bottenheim, J. W., Gallant, A. G. and Brice, K. A. 1986. Measurements of $NO_y$ species at 82° N latitude. *Geophys. Res. Lett.* **13**, 113–116.

Bottenheim, J. W., Barrie, L. A., Atlas, E., Heidt, L. E., Niki, H., Rasmussen, R. A. and Shepson, P. B. 1990. Depletion of lower tropospheric ozone during Arctic spring: The Polar Sunrise Experiment 1988. *J. Geophys. Res.* **95**, 18555–18568.

Braathen, G. O., Hov, Ø. and Stordal, F. 1990. *Arctic atmospheric research station on the Zeppelin Mountain (474 m a.s.l.) near Ny-Ålesund on Svalbard, Lillestrøm.* NILU internal publication OR 85/90.

Curry, J. A. and Radke, L. F. 1993. Possible role of ice crystals in ozone destruction of the lower Arctic troposphere. *Atmos. Environ.* **27A** no.17/18, 2873–2879.

Fan, S. M. and Jacob, D. J. 1992. Surface ozone depletion in Arctic spring sustained by bromine reactions on aerosols. *Nature* **359**, 522–524.

Finlayson-Pitts, B. J., Livingston, F. E. and Berko, H. N. 1990. Ozone destruction and bromine photchemistry at ground level in the Arctic spring. *Nature* **343**, 622–625.

Greenblatt, G. D. and Howard, C. J. 1989. Oxygen atom exchange in the interaction of $^{18}OH$ with several small molecules. *J. Phys. Chem.* **93**, 1035–1043.

Hopper, J. F., Peters, B., Yokouchi, Y., Jobson, B. T., Niki, H., Shepson, P. B. and Muthuramu, K. 1994. Chemical and meteorological observations at ice camp SWAN during Polar Sunrise Experiment 1992. *J. Geophys. Res.* **99**, 25489–25498.

Jobson, B. T., Niki, H., Yokouchi, Y., Bottenheim, J. W., Hopper, F. and Leaitch, R. 1994. Measurements of C2–C6 hydrocarbons during the Polar Sunrise 92 Experiment. *J. Geophys. Res.* **99**, 25355–25368.

Kieser, B. N., Botteheim, J. W., Sideris, T. and Niki, H. 1993. Spring 1989 observations of lower tropospheric chemistry in the Canadian high Arctic. *Atmos. Environ.* **27A**, 2979–2988.

Koppmann, R., Johnen, F. J., Khedim, A., Rudolph, J., Wedel, A. and Wiards, B. 1995, The influence of ozone on light nonmethane hydrocarbons during cryogenic preconcentration. *J. Geophys. Res.* **100**, 11383–11391.

McConnell, J. C., Henderson, G. S., Barrie, L., Bot tenheim, J., Niki, H., Langford, C. H. and Templeton, E. M. J. 1992. Photochemical bromine production implicated in Arctic boundary-layer ozone depletion. *Nature* **355**, 150–152.

DeMore, W. B., Sander, S. P., Golden, D. M., Hampson, R. F., Kurylo, M. J., Howard, C. J., Ravishankara, A. R., Kolc, C. E. and Molina, M. J. 1994. *Chemical kinetics and photochemical data for use in stratospheric modelling.* Jet Propulsion Laboratory Publ. **94–26**, evaluation no. 11.

Nicovich, J. M., Kreutter, K. D. and Wine, P. 1990. Kinetics of the reaction of Cl and Br with ozone. *Int. J. Chem. Kinet.* **22**, 399–414.

Nicovich, J. M. 1996. Kinetics and thermochemistry of the $Cl(^2P_j)+C_2Cl_4$ association reaction. *J. Phys. Chem.* **100**, 680–688.

Oltmans, S. J., Schnell, R. C., Sheridan, P. J., Peterson, R. E., Li, S. M., Winchester, J. W. and Tans, P. P. 1989. Seasonal surface ozone and filterable bromine relationship in the high Arctic. *Atmos. Environ.* **23**, 2431–2441.

Ottar, B. 1987. *Belastung der Arktis durch Emissionen aus anthropogenen Quellen.* VDI Ber. **nr. 608**, 17–46.

Penkett, S. A., Blake, N. J., Lightman, P., Marsh, A. R. W., Anwyl, P. and Butcher, G. 1993. The seasonal variation of nonmethane hydrocarbons in the free troposphere over the north Atlantic ocean: Possible evidence for extensive reaction of hydrocarbons with the nitrate radical. *J. Geophys. Res.* **98**, 2865–2885.

Ramacher, B. 1997. *Messung organischer Spurengase in der arktischen Troposphäre: Hinweise auf einen regionalen halogeninduzierten Ozonabbau.* PhD Thesis, Gerhard-Mercator-University, Duisburg, Germany.

Rudolph, J., Johnen, F. J. and Khedim A. 1986. Problems connected with the analysis of halocarbons and hydrocarbons in the non-urban atmosphere. *Int. J. Environ. Anal. Chem.* **27**, 97–122.

Rudolph, J., Koppmann, R. and Plass-Dülmer, CH. 1996. The budgets of ethane and tetrachloroethene: Is there evidence for an impact of reactions with chlorine atoms in the troposphere? *Atmos. Environ.* **30**, 1887–1894.

Solberg. S., Schmidbauer, N., Semb, A. and Hov, Ø 1996. Boundary-layer ozone depletion as seen in the Norwegian Arctic in spring. *J. Atmos. Chem.* **23**, 301–332.

Taylor, P. H., Jiang, Z. and Dellinger, B. 1993. Determination of the gas-phase reactivity of hydroxyl with chlorinated methanes at high temperature: effects of laser/thermal photochemistry. *Int. J. Chem. Kinet.* **25**, 9–23.

Wallington, T. J., Skewers, L. M. and Siegal, W. O. 1988. Kinetics of the gas phase reaction of chlorine atoms with a series of alkenes, alkynes, and aromatics at 295K. *J. Photochem. Photobio. (A) Chem.* **45**, 167–178.

Yokouchi, Y., Akimoto, H., Barrie L. A., Bottenheim, J. W., Anlauf, K. and Jobson, B. T. 1994. Serial gas chromatographic/mass spectrometric measurements of some volatile organic compounds in the arctic atmosphere during the 1992 Polar Sunrise Experiment. *J. Geophys. Res.* **99**, 25 379–25 389.